Sun Photometer Calibration using high altitude site, Mount Abu

30/11/2019

Calibration and Validation Division
Earth, Ocean, Atmosphere, Planetary Sciences & Applications Area
Space Applications Centre (ISRO)
Ahmedabad – 380 015

Document control and data sheet

1.	Date	December,2019
2.	Title	Sun Photometer Calibration using high altitude site, Mount Abu
3.	Report no.	SAC/EPSA/CVD/CAL-VAL/2016/Cal-02
4.	Report type	Technical
5.	No. of pages	18
6.	No. of references	11
7.	Authors	K. N. Babu, C. Mahesh, and Nandkishor Kumawat
8.	Originating unit	CVD/EPSA
9.	Abstract	This technical report presents the Langley calibration of Sun-photometer using high altitude site (PRL observatory, Mount Abu). The new calibration coefficients derived from 22nd November 2019 is used for updating the original coefficients set in the instrument which are most of the time changed by about ~~3% and in very few cases by ~7% (water vapor channel) due to cloud present in the atmosphere.
10.	Key words	Langley, Calibration, Sun-photometer, Hight altitude, Aerosol
11.	Security classification	Unrestricted
12.	Distribution	Among all concerned

Contents

Summary

Periodic (annual/bi-annual) calibration of sun-photometers and Ozonometers are highly required to have reliable/high-quality measurements on aerosols, columnar atmospheric water, and Ozone concentration. To carry out this exercise with the available units, a high latitude site with less logistic efforts and security is preferred. The Mount Abu site is chosen with few sun-photometers in these initial efforts so as to establish method of calibration for generating the new calibration coefficients. The initial results are encouraging and the new calibration coefficients are derived with highly stable Langley plots. In this measurements and its analysis, we found the instruments have stable filter performance. In total, this exercise of Langley calibration for sun-photometer helps us to update the calibration of sun-photometer. We shall be performing the calibration for all the photometers available in an annual mode using this high altitude site.

1. Objectives

The aerosol optical properties are derived from the sun-photometric measurements. Generally, these photometers are designed for portable, manual measurements and robotic, autonomous measurements. The optical filter channels used in these equipments are subject to degrade with time and hence required periodic calibration using sun as the natural source for calibration at high altitude site. Here we attempted Mount Abu in Rajasthan for doing the calibration exercise for the Microtops-II and CIMEL sun-photometers. This exercise gives us the confidence in doing sun-photometer calibration at PRL observatory, Mount Abu during post south-west monsoon season. As these photometers need at least an annual calibration, we shall perform at this site calibration on annual basis.

2. Introduction

Aerosol particles play a crucial role in global and regional climate change and can affect the general circulation and Earth's radiation budget. In general, aerosols modify the climate through direct and indirect effect. Aerosols exert direct effect through scattering and absorption of incoming and outgoing solar radiation (Satheesh and Ramanathan, 2000; Charlson et al., 1992). Aerosols have and indirect effect through interaction with clouds and hence affect the hydrological

cycle (Ramanathan, et al., 2001). Despite many aerosol studies, aerosol concentrations and optical properties are some of the largest sources of uncertainty in the current assessment and prediction of global climate change. Employing ground-based network of sun-photometer is very useful and accurate way to study the aerosol optical properties and validate the satellite retrieved products. This sun-photometer network has been used to measure the direct and diffuse component of the solar radiation and derive aerosol optical properties. Though the system/instrument works very well but the biggest challenge at present is the lack of their systematic and periodic calibration. Optical depth measurements by the "absolute calibration" method require several precise calibrations for each of the channels band-pass, angular response, and standard lamp-combined with the current satellite-derived top of the atmosphere (TOA) irradiance spectra. All of these calibrations (Miller et al., 2004) are critical to the accuracy of the measurement and must be repeated at regular (annual) intervals. An alternate, much simpler, ad hoc calibration method is possible with the Langley extrapolation (Shaw, 1983), described below. Langley calibrations are free and can be updated every time under a very clear sky condition. The present study reports calibration of the sun-photometer at a high altitude site, Gurushikhar at Mount Abu, Rajasthan.

3. Theory

Light from the sun is seen as an almost a parallel beam of photons. At the top of the atmosphere (TOA) the energy through a plane surface normal to the beam is given by I. The distance from the Earth to the Sun is not constant and therefore I depends on the separation distance, D. The reference solar spectrum, $I_0(\lambda)$ is defined to be the solar irradiance at one astronomical distance. The TOA irradiance for any value of D is given by $I = I_0/D^2$.

A sun photometer measures the directional solar irradiance in discrete wavelength bands along a vector pointing from the instrument detector to the solar disk. The atmosphere both absorbs and scatters light along this vector, and these effects are treated together through the mass extinction cross section k_λ Liou (1980). Because the different scattering and absorbing processes may be assumed to be independent of each other, the total extinction coefficient is a simple sum from all the contributors:

$$k_\lambda = k_A + k_R + k_O + k_N \tag{1}$$

where the terms on the right represent the mass extinction cross sections for aerosol scattering, Rayleigh scattering, Ozone (O_3) absorption, and Nitrogen dioxide (NO_2) absorption.

A parallel beam of radiation, denoted by its irradiance, I_λ, will be reduced in the direction of its propagation by an amount given by

$$dI_\lambda = -k_\lambda \rho I_\lambda ds \tag{2}$$

where k_λ is defined by (1), ρ is the air density, and ds is the differential path length. If k_λ is constant, the classical Beer-Bouguer-Lambert law results:

$$I_\lambda(s_2) = I_\lambda(s_1)e^{-k_\lambda u} \tag{3}$$

where $u = \int \rho ds$ is called the optical thickness or optical path and integration proceeds along the path the ray takes from s_1 to s_2.

In the atmosphere k_λ and ρ are not homogeneous and so the full integration of (2) is required. A reasonable approximation is that the atmosphere is horizontally stratified, and this allows integration of (2) along the vertical axis, z, in a coordinate system on the Earth's surface. Then $ds = sec\theta\ dz$, and

$$I_\lambda(h) = I_{\lambda T}exp(-\int_h^\infty k_\lambda \rho\ sec\ \theta\ dz)$$

where $I_\lambda(h)$ is the irradiance at the observer at height h above sea level, and $I_{\lambda T}$ is the irradiance at the top of the atmosphere (TOA). Integration follows the ray in its refracted path through the atmosphere and, for completeness, must include the curvature of the Earth.

In the case that k_λ is constant through the air column, as in Rayleigh scattering, it can be moved outside the integral. In the cases when it is non-uniform in the column, as for aerosol, O_3, and NO_2, an effective extinction coefficient can be defined. The resulting effective total extinction coefficient is given by $k_\lambda = k_A + k_R + k_O + k_N$ and is defined by

$$\int_h^\infty k_\lambda \rho sec\ \theta\ dz = k_h \int_h^\infty \rho sec\ \theta\ dz = k_h \left[\frac{\int \rho sec\ \theta\ dz}{\int \rho\ dz}\right] \tag{4}$$

The terms with tides are effective mean values that produce the same extinction if uniformly distributed through the atmosphere. The bracketed fraction is defined as the air mass, $m(\theta)$ and is

a function of the zenith angle, θ. When the solar beam is normal to the geoid, m = 1, and the normal atmospheric optical depth (AOD) is defined as

$$k_\lambda = \int_h^\infty k_\lambda\, \rho dz = k \int_h^\infty \rho dz \qquad (5)$$

The resulting formulation for the irradiance becomes

$$I_\lambda(h) = I_{\lambda T} e^{-m(\theta)(k_A + k_R + k_O + k_N)} \qquad (6)$$

which is a working analog to the classical Beer-Bouguer-Lambert equation, (3). Without knowing the vertical and horizontal distribution of the different contributing attenuators, (6) serves as definition of the optical thicknesses which must be derived by observation of the extinction of the solar beam through the atmosphere.

There are two methods to calibrate any radiometer by using the extinction equation 6. These are (1) the absolute method and (2) the Langley method. Most of the difficulties with the absolute calibration methods are bypassed with the Langley method. A good Langley plot requires first and foremost a perfectly clear and cloud free sunset or sun rise. The time 1-2 hours before sunset or after sun rise must be clear and the aerosol loading must be constant. This method eliminates the need for band pass integration, a standard lamp, or any other difficulties in the absolute methods.
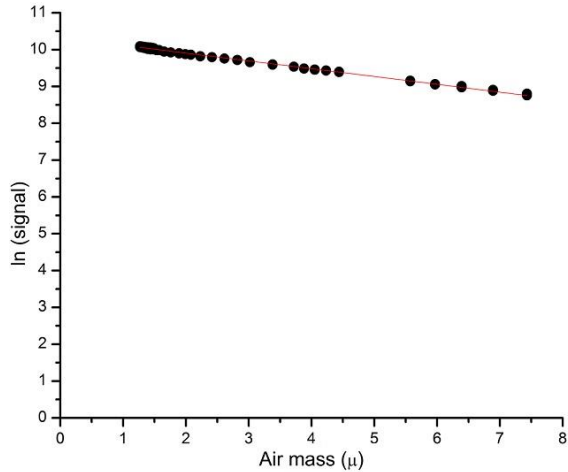
Figure 1: An example of Langley plot, this plot is generated from the measurements which are collected during a calibration campaign (21/11/2019) at Mount Abu. The straight line indicates an ideal Langley plot for a very clear and most suitable venue for the calibration exercise.

4. Instruments and data

A high altitude calibration campaign is envisaged to perform the Langley calibration for the Sun-photometers. One of the mounts in Abu, Rajasthan is considered for performing the calibration exercise during the post south-west monsoon period since this place is easily accessible, allows easy transportation of instruments and moreover this place is known to us. In this calibration campaign total seven sun-photometers are taken for performing Langley calibration out of which five are Microtops-II model of Solar light and two are robotic CIMEL sun-photometer. The instrument serial no. and the date of company calibration are given in Table 1.

Table 1 List of sun-photometer/Ozonometer which are taken for Langley calibration

Instrument type	Instrument Sr. No.	Date of company calibration
Microtops-II/Sun-photometer	22445	09/12/2015
Microtops-II /Sun-photometer	14460	13/04/2009
Microtops-II /Sun-photometer	14459	10/04/2009
Microtops-II /Sun-photometer	22446	09/12/2015
Microtops-II /Ozonometer	19724	16/07/2015
Microtops-II /Ozonometer	19722	16/07/2015
Microtops-II /Ozonometer	19721	16/07/2015
Microtops-II /Ozonometer	10591	08/08/2008
CIMEL/Sun-photometer	977	06/12/2018

The CIMEL CE-318 sunphotometer makes direct spectral solar radiation measurements within a 1.2º full field of view every 15 minutes at eight/nine bands (340, 380, 440, 550, 670, 870, 937, 1020, 1610nm). These solar extinction measurements are then used to compute Aerosol Optical Depth (AOD) at each respective wavelength expect the 937nm channel, which is used for computing the total precipitable water vapor contents in centimeter. Aerosol size distribution, refractive index, and single-scattering albedo are retrieved by using sky radiance (diffused) almucantar measurements and direct sun measurements (Dubovik and King, 2000; Dubovik et al.,

2000) as well as polarized radiances in the sun principal plane (Li et al., 2006, 2007). The total uncertainty in optical depth is about 0.01 to 0.02 (Eck et al., 1999).

The Microtops-II is a hand-held multi-band sunphotometer capable of measuring the aerosol optical depth, total ozone column and optionally the water vapor column (also called precipitable water). Generally one unit is equipped with five (380, 440, 500, 675, 870nm) accurately aligned optical collimators, capable of a full field of view of 2.5^{o}. The theory of measurement and related parameter retrieval from these instruments are given elsewhere 'www.solarlight.com'.

Figure 2 shows the location and the actual field photo of the mount chosen for this purpose. The ground and sky conditions prevailed during these three days is shown in **Figure 2b**. The site altitude is approximately 1700m from mean sea level, the CIMEL sun-photometer is installed at 9:30am and removed at 5:20pm on 21th November 2019 and 9:30am to 4:30pm on 22nd November 2019. While the Microtops-II photometers are operated in synchronization with CIMEL measurements at an interval of 15 minutes and each time their scans are performed. Additionally, Microtops-II sun-photometers are operated at PRL guest house (~1200m altitude) on 22nd November 2019 (Figure-3). The Microtops-II time, location and altitude information are set using Garmin GPS receiver.

Figure 2a: One of the Mount Abu hills (Gurushikhar) chosen for Langley calibration of Sun-photometer
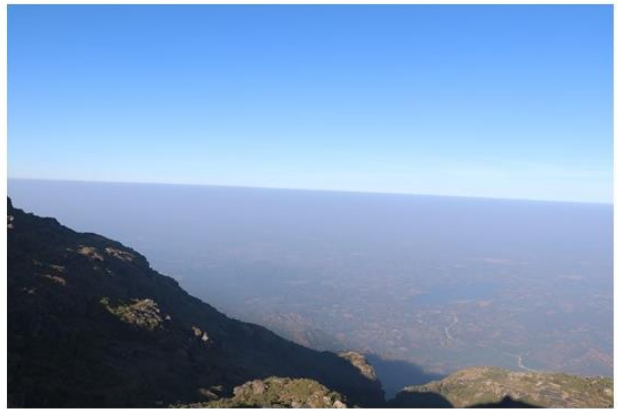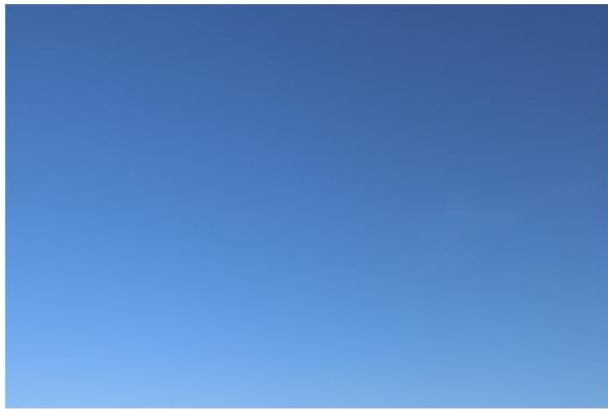
Figure 2b: The sky and ground condition prevailed during the measurement days.

Figure 3: Microtops-II measurements at PRL guest house.

Figure 4: CIMEL measurements near PRL observatory, Gurushikhar at Mount Abu.

5. Results

The observed time series aerosol optical depth is shown in **Figure 5**. The AOD loading is slightly higher on the second day (22nd November 2019) as compared to other two days. From the **Figure 2**, the right panel photo is suggesting a pollution layer over the land surface which is highly influenced by the atmospheric boundary layer and anthropogenic activities. This aerosol loading might be less if the campaign would have been conducted immediately after the monsoon season, as the rains would have cleaned the atmosphere considerably.
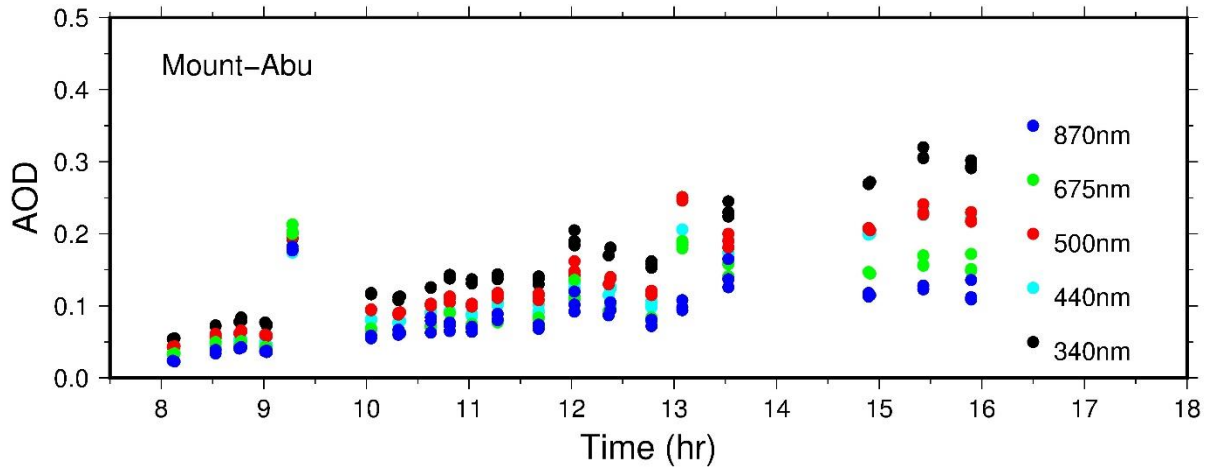
Figure 5: Aerosol optical depth variations at Mount Abu using Microtops-II sun-photometer (S/N.: 22446)

New calibration coefficient for sun-photometer S/N.: 14459
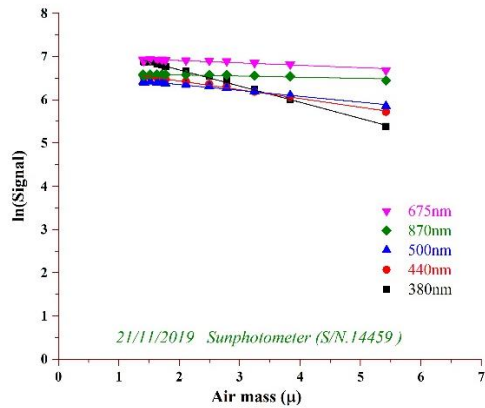
Figure 6: The Langley plot for the sun-photometer S/n. 14459.

Wavelength (nm)	380	440	500	675	870
Old calibration coefficient	7.573	6.926	6.753	7.106	6.647
New calibration coefficient	7.438	6.837	6.622	7.016	6.625
Change in calibration coefficient (%)	1.783	1.285	1.940	1.267	0.331

New calibration coefficient for sun-photometer S/N.: 14460
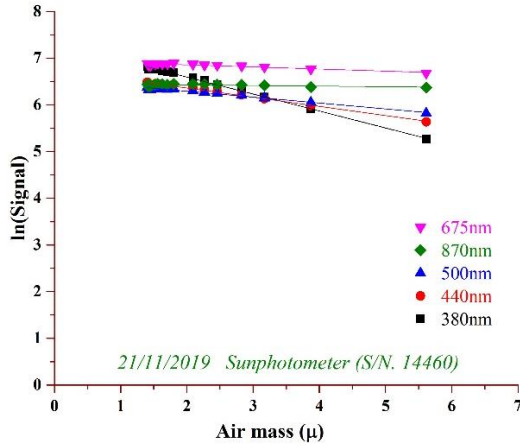
Figure 7: The Langley plot for the sun-photometer S/n. 14460.

Wavelength (nm)	380	440	500	675	870
Old calibration coefficient	7.605	6.904	6.760	7.085	6.632
New calibration coefficient	7.324	6.754	6.547	6.948	6.452
Change in calibration coefficient (%)	3.695	2.173	3.151	1.934	2.714

New calibration coefficient for sun-photometer S/N.: 22445
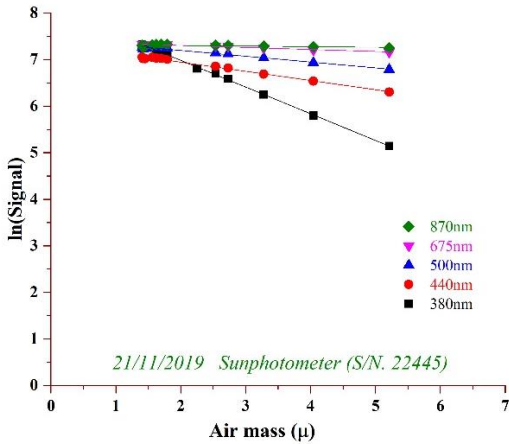
Figure 8: The Langley plot for the sun-photometer S/n. 22445.

Wavelength (nm)	340	440	500	675	870
Old calibration coefficient	8.359	7.467	7.596	7.493	7.440
New calibration coefficient	8.135	7.342	7.450	7.391	7.331
Change in calibration coefficient (%)	2.680	1.674	1.922	1.361	1.465

13

New calibration coefficient for sun-photometer S/N.: 22446
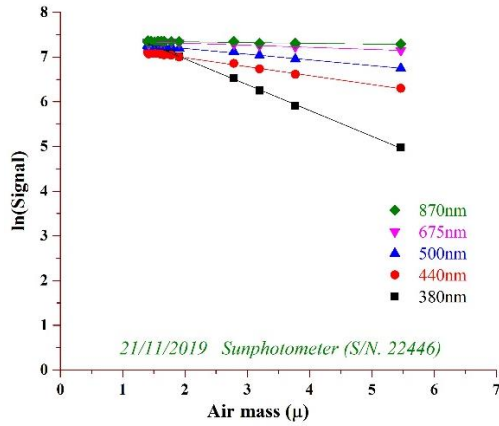
Figure 8: The Langley plot for the sun-photometer S/n. 22446.

Wavelength (nm)	340	440	500	675	870
Old calibration coefficient	8.315	7.504	7.576	7.479	7.451
New calibration coefficient	8.116	7.384	7.449	7.405	7.373
Change in calibration coefficient (%)	2.393	1.599	1.676	0.989	1.047

New calibration coefficient for sun-photometer S/N.: 10591
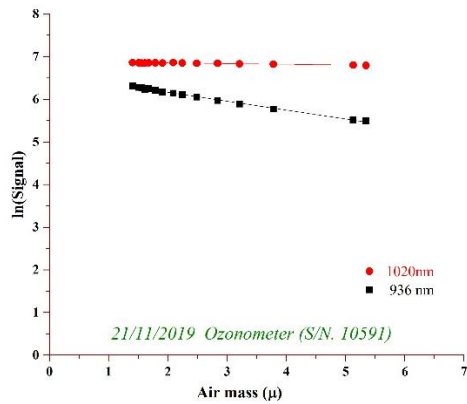
Figure 9: The Langley plot for the sun-photometer S/n. 10591.

Wavelength (nm)	1020	936
Old calibration coefficient	7.063	7.194
New calibration coefficient	6.883	6.581
Change in calibration coefficient (%)	2.548	8.521

New calibration coefficient for sun-photometer S/N.: 19721
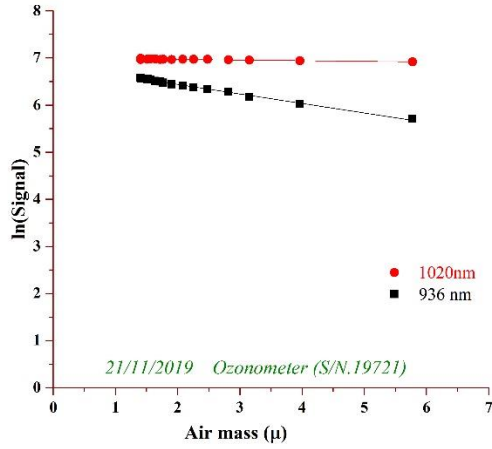
Figure 10: The Langley plot for the sun-photometer S/n. 19721.

Wavelength (nm)	1020	936
Old calibration coefficient	7.122	7.416
New calibration coefficient	6.997	6.843
Change in calibration coefficient (%)	1.755	7.727

New calibration coefficient for sun-photometer S/N.: 19722
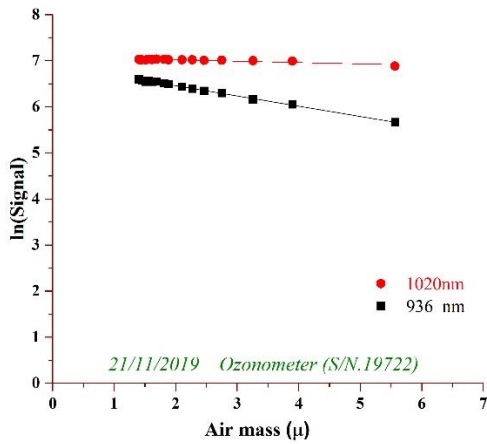
Figure 9: The Langley plot for the sun-photometer S/n. 19722.

Wavelength (nm)	1020	936
Old calibration coefficient	7.098	7.414
New calibration coefficient	7.077	6.903
Change in calibration coefficient (%)	0.296	6.892

New calibration coefficient for sun-photometer S/N.: 19724
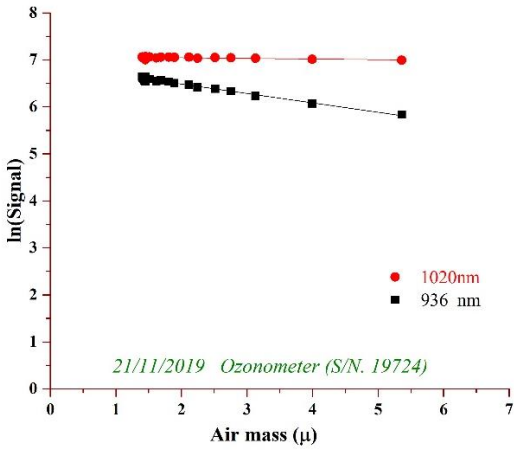
Figure 10: The Langley plot for the sun-photometer S/n. 19724.

Wavelength (nm)	1020	936
Old calibration coefficient	7.110	7.432
New calibration coefficient	7.073	6.887
Change in calibration coefficient (%)	0.520	7.333

New calibration coefficient for sun-photometer S/N.: 1020
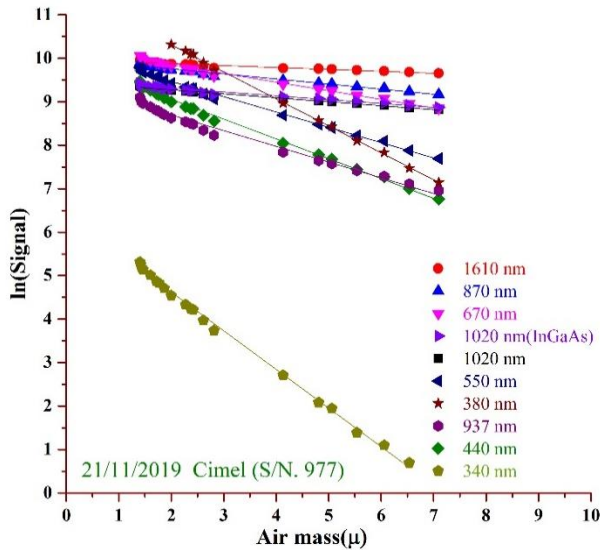
Figure 11: The Langley plot for the CIMEL sun-photometer S/n. 977.

16

Wavelength (nm)	1020	1610	870	670	440	550	1020i	380	340
Old calibration coefficient	12212	21159	20526	25441	18308	22773	12575	102872	504
New calibration coefficient	12710	21236	21844	28270	21454	26334	13194	99637	611
Change in calibration coefficient (%)	-4.08	-0.36	-6.42	-11.12	-17.19	-15.63	-4.92	3.14	-21.26

6. Conclusion

The calibration exercise for sun-photometer is carried out at a nearest high altitude station (Gurushikhar at Mount Abu, Rajasthan). The hilltop at PRL observatory is most suitable with maximum of 2.5% variability in the full day measurements of aerosol optical depth. The basic observations are quite stable and hence the observed Langley plot between air-mass and natural log of signal falls into the most ideal lines. The Langley plots are used to derive the new calibration coefficients for the sun-photometer both hand-held and robotic CIMEL and found very less degradation of company calibration. However these set of instruments are updated with the new calibration coefficient which are obtained in the calibration campaign. This exercise gives us the confidence in doing sun-photometer calibration at PRL observatory, Mount Abu during post south-west monsoon season. As these photometers need atleast an annual calibration, we shall perform at this site calibration on annual basis.

7. References

Charlson, R.J., Schwartz, S.E., Hales, J.M., Cess, R.D., Coakley, J.A., Hansen, J.E., and Hoffmann, D.J. (1992), Climate Forcing by Anthropogenic Aerosols. *Science*. 255, 423-430.

Dubovik, O., and M. D. King (2000), A flexible inversion algorithm for the retrieval of aerosol optical properties from Sun and sky radiance measurements, J. Geophys. Res., 105, 20,673 – 20,696, doi:10.1029/2000JD900282.

Dubovik, O., A. Smirnov, B. N. Holben, M. D. King, Y. J. Kaufman, T. F. Eck, and I. Slutsker (2000), Accuracy assessments of aerosol optical properties retrieved from AERONET sun and sky radiance measurements, J. Geophys. Res., 105, 9791– 9806, doi:10.1029/2000JD900040.

Eck, T. F., B. N. Holben, J. S. Reid, O. Dubovik, A. Smirnov, N. T. O'Neill,I. Slutsker, and S. Kinne (1999), Wavelength dependence of the opticaldepth of biomass burning, urban, and desert dust aerosols, J. Geophys.Res., 104, 31,333– 31,349, doi:10.1029/1999JD900923.

Li, Z., P. Goloub, C. Devaux, X. F. Gu, J. L. Deuze, Y. L. Qiao, and F. S. Zhao (2006), Retrieval of aerosol optical and physical properties from ground-based spectral, multi-angular and polarized Sun photometer measurements, Remote Sens. Environ., 101, 519– 533.

Li, Z., P. Goloub, L. Blarel, B. Damiri, T. Podvin, and I. Jankowiak (2007), Dust optical properties retrieved from ground-based polarimetric measurements, Appl. Opt., 46, 1548– 1553, doi:10.1364/AO.46.001548.

Liou K., (1980), An Introduction to Atmospheric Radiation, International Geophysics Series, vol. 26, Academic press, San Diego, C.A.

Miller,M. A., M.J. Bartholomew, and R.M. Reynolds, (2004) the accuracy of marine shadow – band sun photometers of aerosol optical thickness and Angstrom exponent, Journal of Atmospheric and Oceanic Technology, 21(3), 397-410.

Ramanathan, V., Crutzen, P.J., Kiehl, J.T., Rosenfeld, D., 2001. Aerosol, climate, and the hydrological cycle. *Science*.294, 2119–2124.

Satheesh, S.K. and Ramanathan, V., (2000), Large differences in tropical aerosol forcing at the top of the atmosphere and Earth's surface. *Nature*. 405, 60–63.

Shaw, G.E., (1983) Sun Photometry, Bulletin of American Meteorological Society, 64(1), 4-10.